

1           **Hillsborough Bay Inflow Modification Study: An Application of the**  
2                                   **Tampa Bay Coastal Ocean Model**

3                                   by

4                   **Jing Chen<sup>1</sup>, Robert H. Weisberg<sup>1</sup>, Yonggang Liu<sup>1</sup>, Lianyuan Zheng<sup>1</sup>**

5  
6   <sup>1</sup>College of Marine Science, University of South Florida, St. Petersburg, FL 33701, USA

7  
8  
9                                   Manuscript submitted to ECSS

10   (Special Issue on Advanced (numerical and observational) Techniques in Mixing and Transport  
11                                   in Estuarine and Coastal Waters under Extreme Conditions)

12                                   July 29, 2022

13  
14  
15   Correspondence to: Yonggang Liu ([yliu@usf.edu](mailto:yliu@usf.edu))

16                                   Jing Chen ([jchen15@usf.edu](mailto:jchen15@usf.edu))

17  
18   Final published version:

19   Chen, J., Weisberg, R.H., Liu, Y., Zheng, L., (2023), [Hillsborough bay inflow modification](#)  
20   [study: An application of the Tampa Bay Coastal Ocean Model](#), *Estuarine, Coastal and Shelf*  
21   *Science*, 108213, <https://doi.org/10.1016/j.ecss.2023.108213>

24 **Abstract**

25

26           With a large salinity gradient existing between the rivers and the ocean, the saline  
27 environment of an estuary is crucial to its ecosystem functionality. For Tampa Bay, the Howard  
28 F. Curren Advanced Wastewater Treatment Plant (HFCAWTP) presently yields an outflow of  
29 nearly freshwater to the Hillsborough Bay portion of Tampa Bay. In order to estimate the  
30 potential impact that the removal of this outflow may have on the salinity and flow fields of  
31 Hillsborough Bay, as part of the Tampa Augmentation Project, both numerical circulation model  
32 and Knudsen theorem applications are made. The numerical model study compares the  
33 instantaneous and nontidal, mean estuarine circulation and salinity distributions for the  
34 Hillsborough Bay on the basis of the HFCAWTP outflow being either included with, or excluded  
35 from, the freshwater inflows. It is found that the potential reduction of the treated reclaimed  
36 water inflow to the bay from the HFCAWTP will not significantly affect the circulation or the  
37 salinity distributions of Hillsborough Bay or of the larger Tampa Bay. The estimation through a  
38 Knudsen theorem application shows an 0.13 psu increase of salinity after remove the HFCAWTP  
39 outflow when averaged within Hillsborough Bay. Thus, both approaches demonstrate that the  
40 effects of HFCAWTP outflow removal are very small when compared with variations that occur  
41 naturally.

42 **Keywords** Tampa Bay, Coastal Ocean Circulation Model, environmental perturbations,

43 Knudsen theorem

44

45

46

47

48 **1 Introduction**

49 Tampa Bay, like many estuaries near metropolitan areas, has a variety of competing uses.  
50 Ecologically, it provides nursery and habitat for estuarine, coastal and deeper-water fishes and  
51 other marine organisms, while with a surrounding population of some four million people, it also  
52 serves as a recreational resource, a depository for treated municipal wastes, and with the only  
53 deep-water port on Florida's west coast, it services the marine transportation industry. Thus, of  
54 importance for bay management is the determination of how the bay may respond to altered  
55 utilizations.

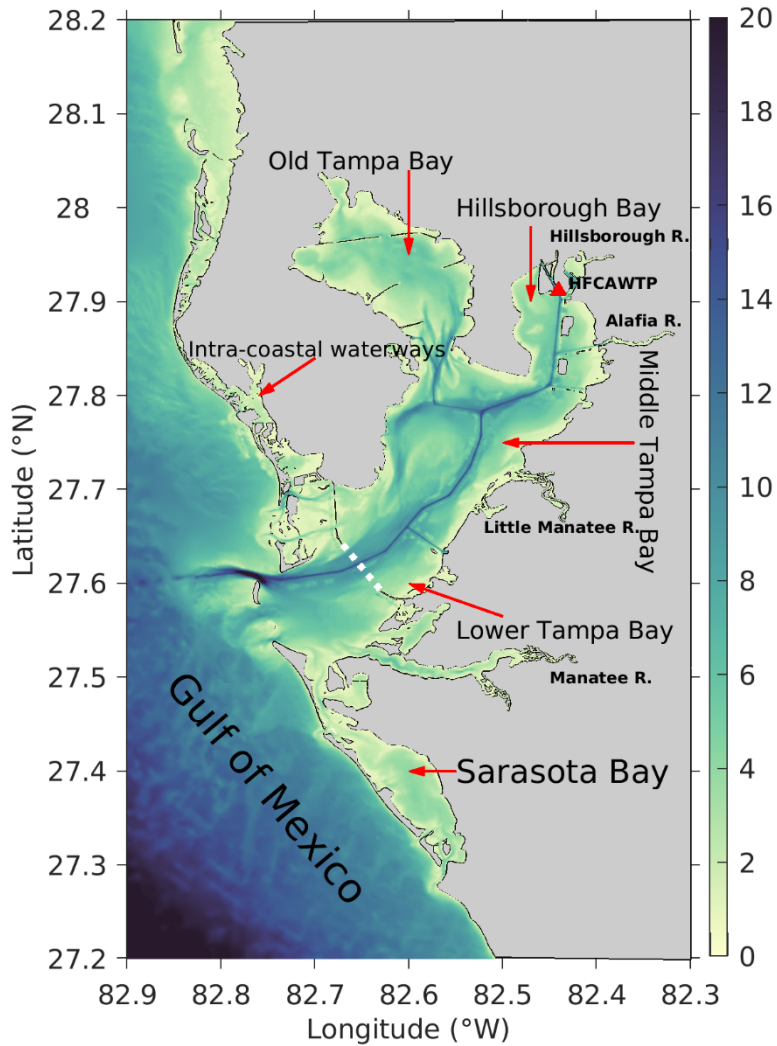
56 With large salinity differences between the rivers (0 psu) and the ocean (~35 psu), the  
57 salinity distribution, a controlling factor for many marine organisms (e.g., Gunter, 1961), is  
58 critical component of the estuarine ecosystem. The spatial and temporal distribution of an  
59 estuary's salinity field is mainly controlled by river discharge and tides (e.g. Prandle, 1985;  
60 Simpson et al., 1990; Geyer, 1993; Xia et al., 2011) and by winds (e.g. Weisberg, 1976; Chen  
61 and Sanford, 2009; Aristizábal and Chant, 2015; Giddings and MacCready, 2017; Kang et al.,  
62 2017; Zhu et al., 2020). It can also be affected by man-made structures (e.g. Das, 2010; White et  
63 al., 2018) and by runoff regulation (Qiu and Zhu, 2013). Variations in the abundance of estuarine  
64 organisms may occur through physical attributes of habitat (such as the salinity and flow fields)  
65 that vary with freshwater inflows (e.g., Kimmerer, 2002; Gillanders & Kingsford 2002).

66 Here we apply a very high resolution, unstructured grid (a triangular grid in this case),  
67 numerical circulation model to assess the results of a fresh water inflow modification proposed  
68 for the Hillsborough Bay portion of Tampa Bay by the City of Tampa, FL Tampa Bay  
69 Augmentation Project (TAP). TAP intends to supply additional potable water by using highly

70 treated reclaimed water from the City's Howard F. Curren Advanced Wastewater Treatment  
71 Plant (HFCAWTP) that is presently being released into Tampa Bay.

72         The location of the present HFCAWTP outflow relative to Hillsborough Bay and the  
73 entirety of Tampa Bay, the adjacent Gulf of Mexico and the various natural river inflows are  
74 shown in Figure 1. The numerical model to be applied is the Tampa Bay Coastal Ocean Model  
75 (TBCOM) that includes the entire Tampa Bay vicinity and its adjacent Gulf of Mexico with  
76 horizontal resolution as fine as 20 m to include Tampa Bay, Sarasota Bay, the intra-coastal  
77 waterway and all of the inlets connecting these water bodies with each other and with the Gulf of  
78 Mexico, as shown in Figure 2. To assess the potential effects of the HFCAWTP outflow  
79 removal, we compare the instantaneous and non-tidal, mean estuarine circulation and salinity  
80 distributions for the Hillsborough Bay sub-region of Tampa Bay with either the HFCAWTP  
81 outflow being included, or excluded from, the freshwater inflows.

82         The remainder of the paper is as follows. Section 2 discusses the development of  
83 TBCOM and why it is an appropriate tool for this study. Section 3 describes the experimental  
84 design of the study. The results of numerical experiments are discussed in section 4. A more  
85 simplified estimation analysis using the Knudsen theorem to back up the numerical analyses is  
86 provided in section 5. Section 6 offers a summary and conclusions.



87  
 88 **Figure 1.** The major structural features and subregions of Tampa Bay, with color-coded  
 89 bathymetry (units in m). The HFCAWTP location is in the upper right.

90

91 **2 Tampa Bay Coastal Ocean Model**

92 TBCOM downscales from the deep-ocean, across the continental shelf and into the  
 93 estuary by nesting the unstructured grid, Finite Volume Community Model (FVCOM, e.g., Chen  
 94 et al., 2003), which has been successfully applied in estuarine and coastal systems (e.g., Yuan et  
 95 al., 2015, Niu et al., 2018, Xia et al., 2020, Sahoo et al., 2021, Kang and Xia, 2022), into the West  
 96 Florida Coastal Ocean Model (WFCOM, e.g., Zheng and Weisberg, 2012, as modified by

97 Weisberg et al., 2014). WFCOM covers continental shelf region of the eastern Gulf of Mexico,  
98 from just west of the Mississippi River Delta to just south of the Florida Keys, by nesting  
99 FVCOM in the Gulf of Mexico Hybrid Coordinate Model (GOM-HYCOM, e.g., Chassignet et  
100 al., 2009). By deriving its deep-ocean boundary values of variables (including tides) from the  
101 GOM HYCOM and its continental shelf forcing from WFCOM, TBCOM further increases the  
102 grid resolution to resolve the finer details of the Tampa Bay vicinity, yielding a three-  
103 dimensional, density dependent estuarine model that is both fully connected to the adjacent  
104 ocean and includes the geometrical complexity of the shoreline and bathymetry as well as the  
105 ability to flood and dry.

106         Given that estuaries are mixing regions for freshwater and seawater, salinity is a primary  
107 variable for determining how flow modifications may impact estuarine ecology. Conceptual  
108 mixing arguments demonstrate the need for very high-resolution models with flooding and  
109 drying capabilities for considering salinity variations, especially in the shallowest nearshore  
110 regions. With fresh water readily mixed over shallow depths, dilution is proportional to depth;  
111 hence, if either depth variations are not resolved by model, or the exclusion of flooding-drying  
112 necessitates a minimum depth for model stability (e.g., Zheng et al., 2003, Chen et al., 2008),  
113 then it is not possible to estimate shallow water salinity variations owing to freshwater inflow  
114 modifications.

115         The starting point for TBCOM was the work of Weisberg and Zheng (2006) followed by  
116 those of Zhu et al. (2015a, b, c). The first of these applied FVCOM to Tampa Bay and  
117 demonstrated the utility of using an unstructured grid model for simulating the circulation. By  
118 further increasing horizontal resolution, the next three applications studied the effects of  
119 deepening and widening the shipping channels, diagnosed the point by point salt balances

120 throughout the bay and the flushing times for the bay as a whole and for its sub-regions,  
121 respectively. Chen et al. (2019), carried these studies a step farther by diagnosing the point by  
122 point momentum balances throughout the bay. The grid configuration used in all but the first of  
123 these aforementioned works is given in Figure 2.

124         With the initial applications to Tampa Bay all being diagnostic hindcasts, the next step  
125 was to combine the Tampa Bay grid with WFCOM to produce a daily, automated nowcast and  
126 forecast model available on the internet for public and other uses. As presently configured,  
127 TBCOM has 219,337 triangular elements with 115,369 nodes in the horizontal and 11 uniformly  
128 distributed  $\sigma$ -layers in the vertical (where  $\sigma$ -layers are terrain following layers that expand or  
129 contract proportionally with varying water depth). The horizontal resolution (Figure 2) gradually  
130 increases from about 8.5 km along the open boundary to about 200 m near the coast, and as fine  
131 as 20 m within Tampa Bay. With such a high resolution, TBCOM uniquely resolves the main  
132 shipping channel and all of the inlets and waterways connecting the Tampa Bay, Sarasota Bay  
133 and the Intra-Coastal Waterway with each other and with the adjacent Gulf of Mexico. Land  
134 elevation and bathymetry data sets are from NOAA and USGS (Hess, 2001). Along the open  
135 boundary, hourly values of sea level, velocity, temperature and salinity are provided along the  
136 open boundary by WFCOM, interpolated to the open boundary nodes and then smoothly merged  
137 with those values from TBCOM over a transition zone consisting of the 10 outermost nodes.  
138 Given that WFCOM already includes tides, no additional tidal forcing is required for TBCOM.

139         For each daily nowcast/forecast run, the initial conditions are taken from the previous  
140 day's hindcast result. At the surface, TBCOM is forced by momentum (winds) and heat fluxes  
141 provided by the NOAA NCEP NAM with spatial and temporal resolutions of 12 km and 6 hours,  
142 respectively. Recognizing that the net surface heat flux may be biased (e.g., Virmani &

143 Weisberg, 2005) and to correct for possible systematic temperature drifts, we relax the modeled  
144 sea surface temperature (SST) to the satellite remote sensing derived Operational Sea Surface  
145 Temperature and Sea Ice Analysis (OSTIA) product (Donlon et al., 2012). Finally, daily river  
146 discharges are downloaded from the USGS website, and the river inflow sites are also shown in  
147 Figure 2. With this TBCOM nowcast/forecast system construct completed in August 2017,  
148 Hurricane Irma provided a reality check of the extreme case the following month. Chen et al.  
149 (2018) describes the TBCOM performance for this initial, unplanned proof of concept  
150 demonstration. The veracity of TBCOM has also been evaluated in under normal conditions  
151 (Chen 2021) using in situ observations.

152 Publicly available TBCOM outputs have been posted continually since September 2017  
153 at <http://ocgweb.marine.usf.edu/~tbn/index.html>. These include a one day hindcast and 3.5 days  
154 of forecasts for surface currents and sea levels over the entire domain, plus sea level time series  
155 at selected sites. Subsequently added (in collaboration with colleagues at the Florida Fish &  
156 Wildlife Commission, Florida Wildlife Research Institute) was a red tide tracking tool to forecast  
157 where observed *Karenia brevis* red tide cell concentrations would be transported to over the next  
158 3.5 days (Liu et al. 2018).

159 Along with these hurricane storm surge and red tide applications, TBCOM also played an  
160 important role in tracking the pollutant plume that emanated from an emergency release of water  
161 from the defunct Piney Point orthophosphate stack in April 2021 (e.g., Liu et al. 2021; Beck et  
162 al. 2022). TBCOM also helped to guide dead fish cleanup operations by Pinellas County during  
163 the major red tide event that ensued subsequent to the Piney Point release. Other recent  
164 applications include the works of Xie et al. (2019, 2021) describing the precision of GPS  
165 observations on a spar buoy anchored at the mouth of Tampa Bay.



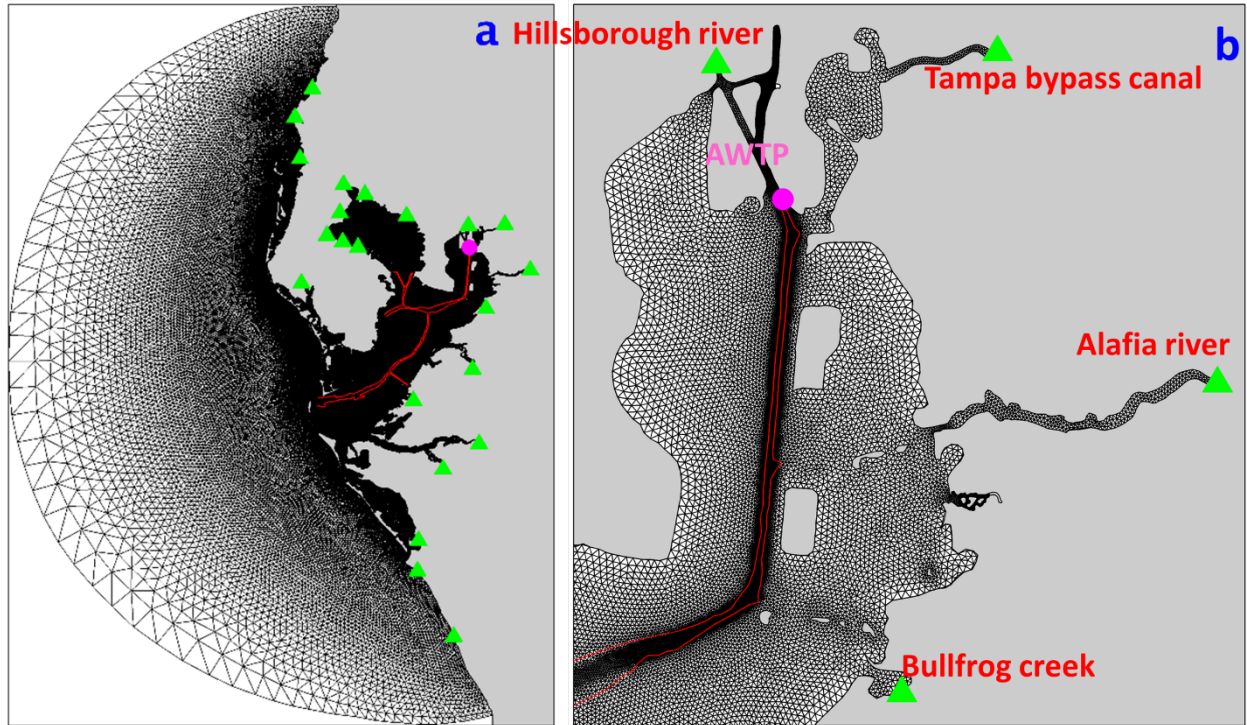
166

### 167 **3 Experimental Design**

168           To investigate the influence of the potential reduction of the treated reclaimed water  
169 inflow from the HFCAWTP, two sets of numerical model simulations (dry season: March 1,  
170 2018 to May 31, 2018; wet season: July 1, 2018 to September 30, 2018) were run. Each set  
171 included two simulations, one with the HFCAWTP outfall discharge flow, the other without the  
172 discharge. The initial conditions were TBCOM hindcast results (February 28 and June 30, 2018).  
173 Given the limited area extent of Hillsborough Bay and its mostly shallow depths, baroclinic  
174 adjustments to fresh water inflows there occur rapidly. Thus, we conservatively discarded the  
175 first month of simulations (March 1 to March 31, 2018, and July 1 to July 31, 2018) by which  
176 time the salinity field was fully adjusted to the new forcing conditions of the HFCAWTP outfall  
177 being either on or off and used the subsequent two months (April 1, 2018 to May 31, 2018, and  
178 August 1, 2018 to September 30, 2018) for analyses.

179           Of the 22 river inflow sites to the TBCOM domain (Figure 2a), Hillsborough Bay hosts  
180 four of these: the Hillsborough and Alafia rivers, the Tampa Bypass Canal, and Bullfrog Creek  
181 (Figure 2b), with averaged discharge rates during the model simulation period of about 8.7  
182 (although for most of this time the discharge is 0.0), 7.88, 2.1, and 0.8 m<sup>3</sup>/s, respectively in the  
183 dry season, and about 27.3, 27.3, 5.7, and 2.9 m<sup>3</sup>/s, respectively in the wet season. The realistic  
184 time series of river fluxes were used in the experiments.

185

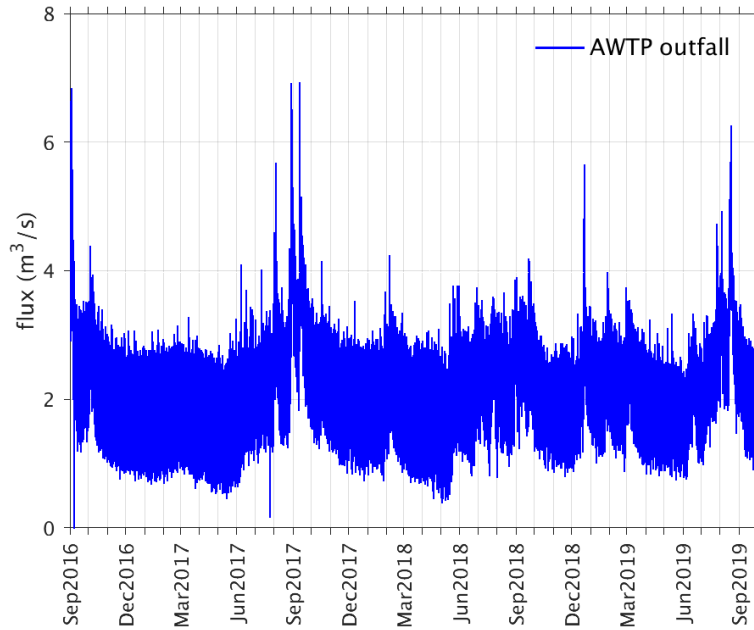


186

187 **Figure 2.** The locations (green triangles) of river discharge in the TBCOM model domain (a) and  
 188 a zoomed view of the Hillsborough Bay subregion (b). The pink dots represent the location of  
 189 the HFCAWTP outfall. The red lines indicate the shipping channel.

190

191 In comparison with the natural river inflows to Hillsborough Bay, the discharge record  
 192 for the HFCAWTP outfall is shown in Figure 3. These discharge rates range from 1 to 3 m<sup>3</sup>/s  
 193 over most of the record, so we chose 3 m<sup>3</sup>/s (106 cfs) as the HFCAWTP discharge to use in the  
 194 simulation. The salinity of this HFCAWTP outfall was set as 1 psu based on the observations  
 195 provided. Whereas the choice of 3 m<sup>3</sup>/s is larger than the mean (that visually looks closer to 2  
 196 m<sup>3</sup>/s), there are times of larger discharge, so this choice seems reasonable.



197

198 **Figure 3.** The discharge record for the Howard F. Curren Advanced Wastewater Treatment Plant  
 199 outfall into Hillsborough Bay.

200

201 **4 Results**

202 The nontidal, near-surface circulations during the wet season (Figures 4a and 4b) show a  
 203 generally directed outflow, whereas by virtue of the vertically integrated salinity compensation  
 204 to the pressure gradient (baroclinic pressure gradient), the near-bottom circulations (Figure 4d  
 205 and 4e) show a generally directed inflow. The mean flow distribution complexities, both at the  
 206 surface and bottom, reflect the geometrical complexities of the Hillsborough Bay and its main  
 207 shipping channel. Consistent with, and as explained in the earlier work of Weisberg and Zheng  
 208 (2006), there is a general convergence of flow into the main shipping channel at the surface,  
 209 where the surface dynamic height tends to have a local minimum, and a divergence away from  
 210 the main shipping channel near the bottom. Thus, at least over the deeper portion of the bay, the  
 211 mean circulation exhibits a classical two-layered estuarine circulation pattern, as expected. The

212 differences of the nontidal circulations between the two experiments are shown in Figures 4c and  
213 4f. No substantive differences are seen. Quantitatively, the differences between the average  
214 current speeds with and without the outfall within a 200 m radius of HFCAWTP amount to 3.6  
215 cm/s at the surface and 0.6 cm/s at the bottom (Table 1). These reduce further to less than 1 cm/s  
216 over a 3000 m radius, which is near the detection limit of a velocity measuring device such as an  
217 acoustic Doppler current profiler (ADCP).

218 The influences of HFCAWTP on the average circulations for the dry season are shown in  
219 Figure 5. Whereas the differences for the nontidal circulations between the experiments with and  
220 without the HFCAWTP outfall during the dry season are slightly larger when compared with the  
221 wet season, these differences are still quite small (Table 1).

222 The non-tidal salinity distributions during wet season within the near surface (Figures 4a  
223 and b) and near bottom sigma layers (Figures 4d and e) follows the circulation. Salinity generally  
224 decreases from the Hillsborough Bay mouth to its head, both at the near surface and near bottom,  
225 but with the up-estuary advection of salt being most evident near the bottom along the main  
226 shipping channel. The differences of the nontidal salinity between the two experiments are  
227 shown in Figures 4c and 4f. As with the nontidal circulation, no substantive differences are  
228 observed. The salinity in Hillsborough Bay increases when the HFCAWTP outfall is removed,  
229 but this increase, over most of the bay, is quite small. Quantitatively, the differences between the  
230 average salinity over the whole bay with and without the outfall amount to 0.21 psu at the  
231 surface and 0.16 psu at the bottom (Table 2). The increase is a bit larger to 0.36 psu at the  
232 surface and 0.18 psu at the bottom over a 1000 m radius. Immediately adjacent to the  
233 HFCAWTP outfall (200 m radius), the salinity increases by about 0.75 psu at the surface and  
234 0.18 psu at bottom.

235 **Table 1.** Time and space average change of current speed within different distance away from  
 236 the HFCAWTP.

Radius from HFAWTP	Difference of speed (wet season)		Difference of speed (dry season)	
	Surface (cm/s)	Bottom (cm/s)	Surface (cm/s)	Bottom (cm/s)
200m	3.6	0.6	5.6	1.6
500m	2.0	0.3	3.8	1.0
1000m	1.4	0.2	2.7	0.8
3000m	0.5	0.1	1.1	0.3
Hillsborough bay	0.2	0.0	0.7	0.2

237  
 238 For the dry season, the influence of HFCAWTP on the average salinity is increased due  
 239 to the decrease of the natural river influxes (Figure 5). Whereas the differences for the average  
 240 salinity between the experiments with and without the HFCAWTP outfall during the dry season  
 241 are slightly larger when compared with those during the wet season, these differences are still  
 242 quite small (Table 2).

243  
 244  
 245  
 246  
 247  
 248 **Table 2.** Time and space average change of salinity within different distance away from the  
 249 HFCAWTP.

Radius from HFAWTP	Difference of salinity (wet season)		Difference of salinity (dry season)	
	Surface (psu)	Bottom (psu)	Surface (psu)	Bottom (psu)
200m	0.75	0.18	2.38	0.48
500m	0.46	0.18	1.52	0.48
1000m	0.36	0.18	1.11	0.44
3000m	0.27	0.17	0.73	0.43
Hillsborough bay	0.21	0.16	0.46	0.33

250  
 251

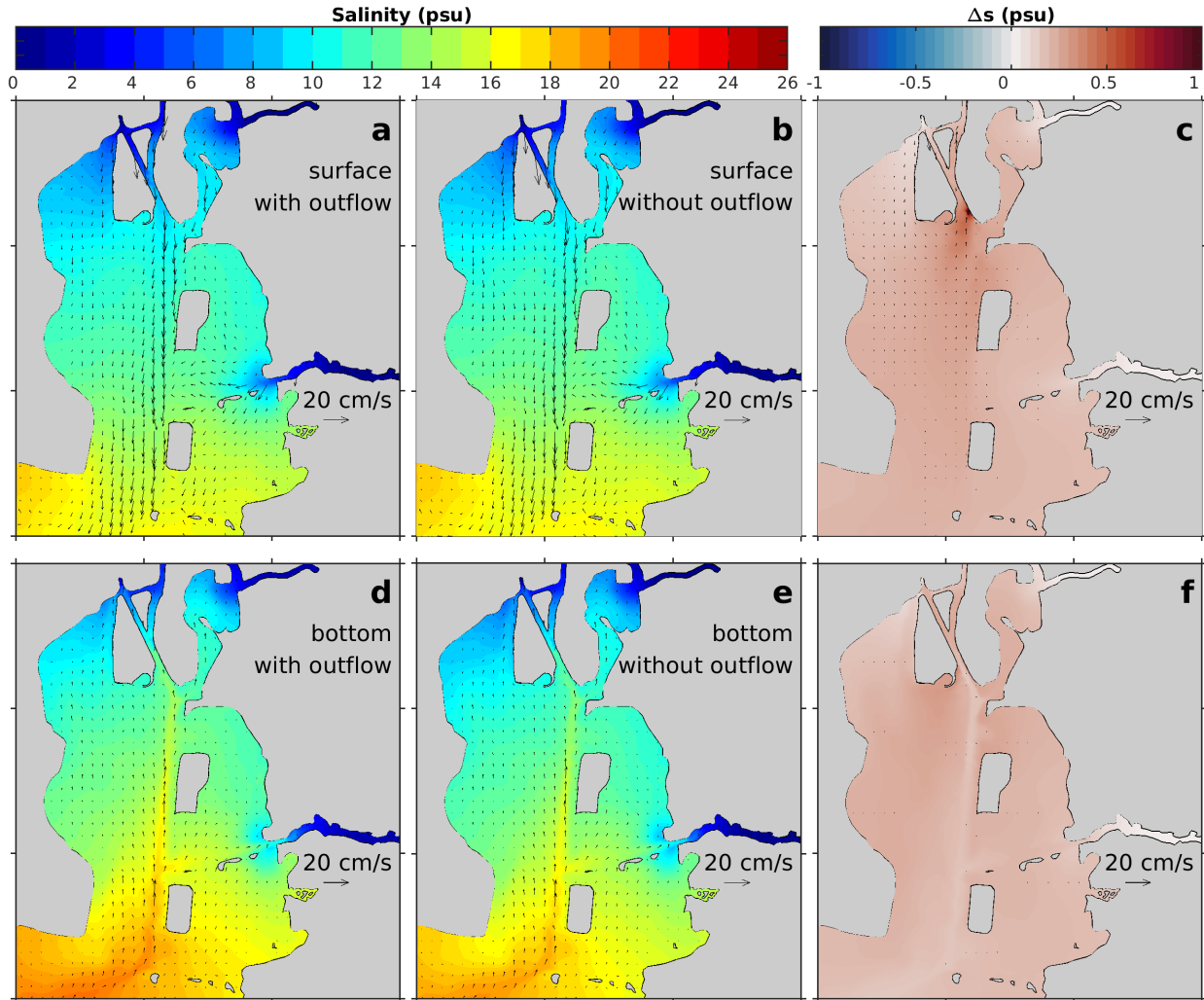
252 Recognizing that instantaneous and record length-averaged (61-day average) distributions  
253 of nontidal current and salinity may differ, the analyses also include an examination of the  
254 instantaneous currents and salinity. The distributions of the near surface instantaneous currents  
255 and salinity throughout Hillsborough Bay sampled over about one semidiurnal tidal cycle either  
256 with or without the HFCAWTP outfall, and their differences are shown in Figures 6 and 7,  
257 respectively, for the wet season simulation. The instantaneous current is much stronger than the  
258 record length-averaged current because the record length-averaging filters out the tidal current  
259 variations that generally are much stronger than the non-tidal currents (by gravitational  
260 convection). In both simulations (with or without the HFCAWTP outfall), the isohalines move  
261 up and down estuary with the tidal current. Thus, at any given location, the salinity usually varies  
262 by a few psu. While not shown, salinity also varies on the time scales of weather frontal passages  
263 (days to weeks) as well as seasonally. All of these natural variations (by tides, winds and rivers)  
264 have salinity effects that are much larger than the small effects found for the cessation of the  
265 HFCAWTP outflows.

266 One additional point that requires mention is that TBCOM, as presently run, does not  
267 include evaporation and precipitation. Consequently, TBCOM tends to underestimate salinity  
268 (i.e., evaporation – precipitation tends to increase the salinity of Tampa Bay). This effect results  
269 in a systematic error for salinity, but one that is on a spatial scale much larger than the  
270 HFCAWTP outflow scale. In other words, the omission of evaporation-precipitation in the  
271 present TBCOM simulation does not influence our findings on the salinity variations due to a  
272 cessation of the HFCAWTP outflow in any way.

273

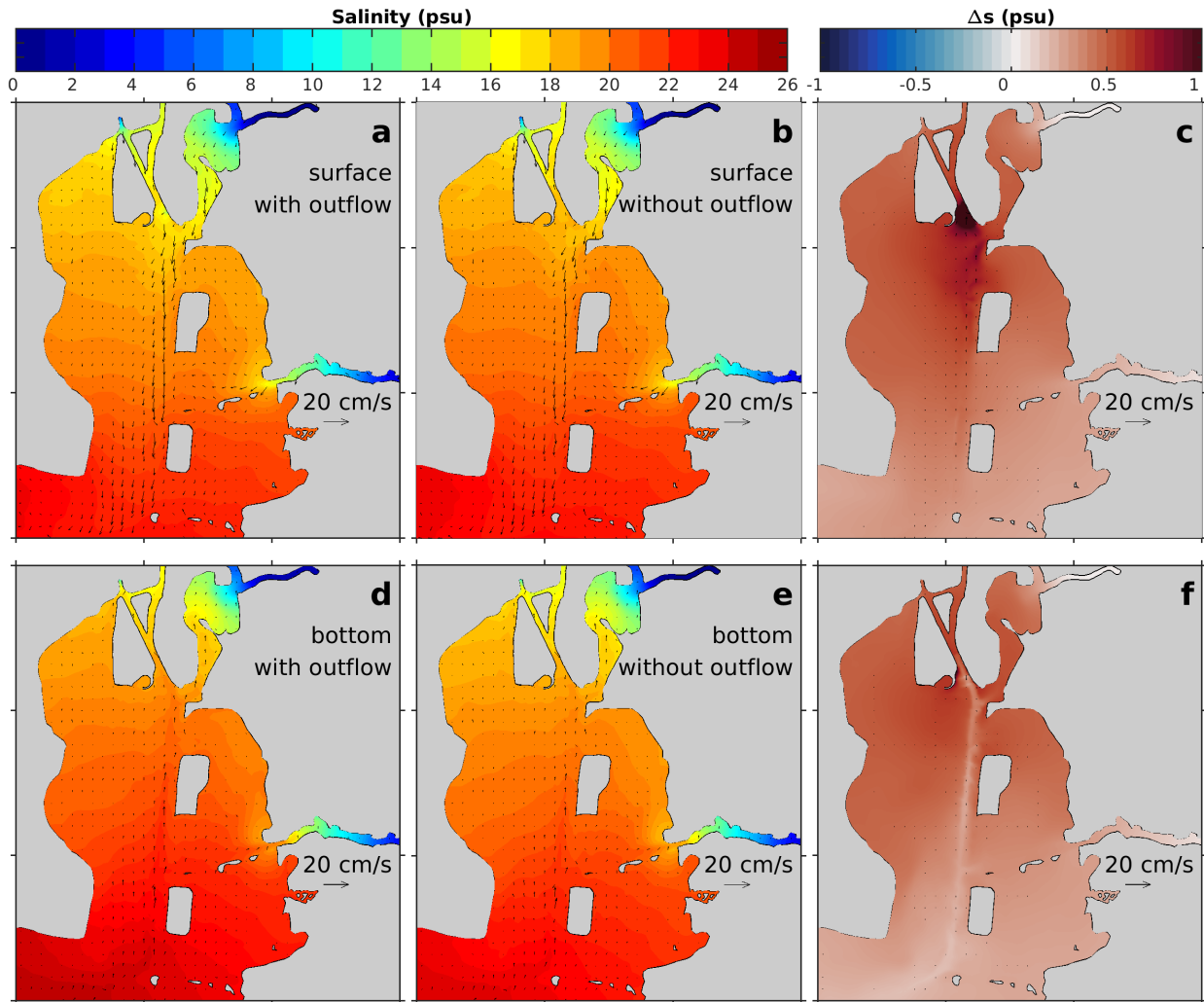
274

275



276

277 **Figure 4.** Model results of nontidal (61-day average) currents (arrows) and salinity (color coded)  
 278 during the wet season. Distributions of the nontidal currents and salinity throughout  
 279 Hillsborough Bay at the near surface (a, b) and the near bottom (d, e) layers for the experiment  
 280 either with the HFCAWTP outfall (left column), or without the HFCAWTP outfall (middle  
 281 column). The differences of the average currents and salinity between the two experiments (with  
 282 and without the HFCAWTP outflow) in the near surface (c) and the near bottom (f) layers.



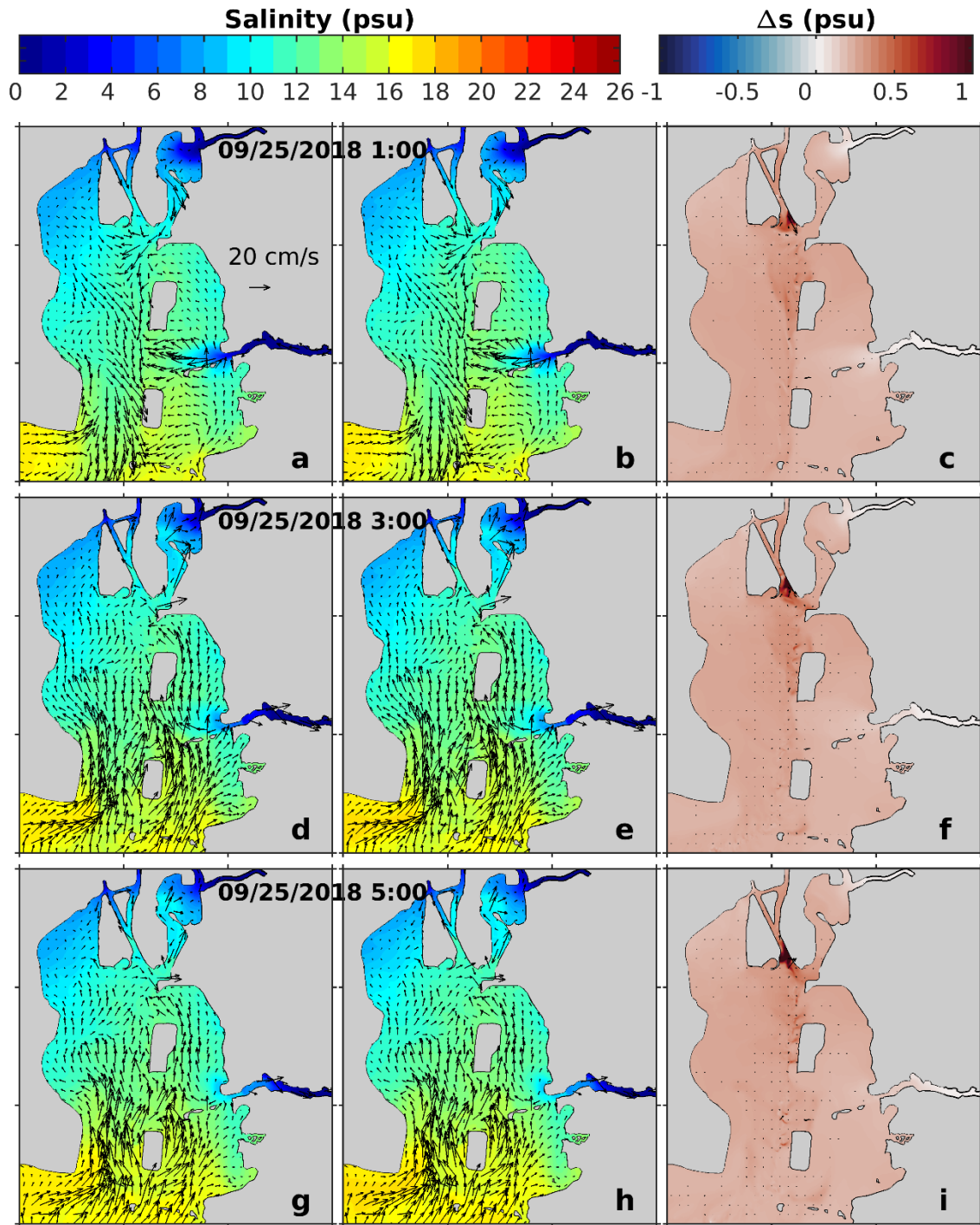
283

284 **Figure 5.** Same as Figure 4 but for the dry season.

285

286





287

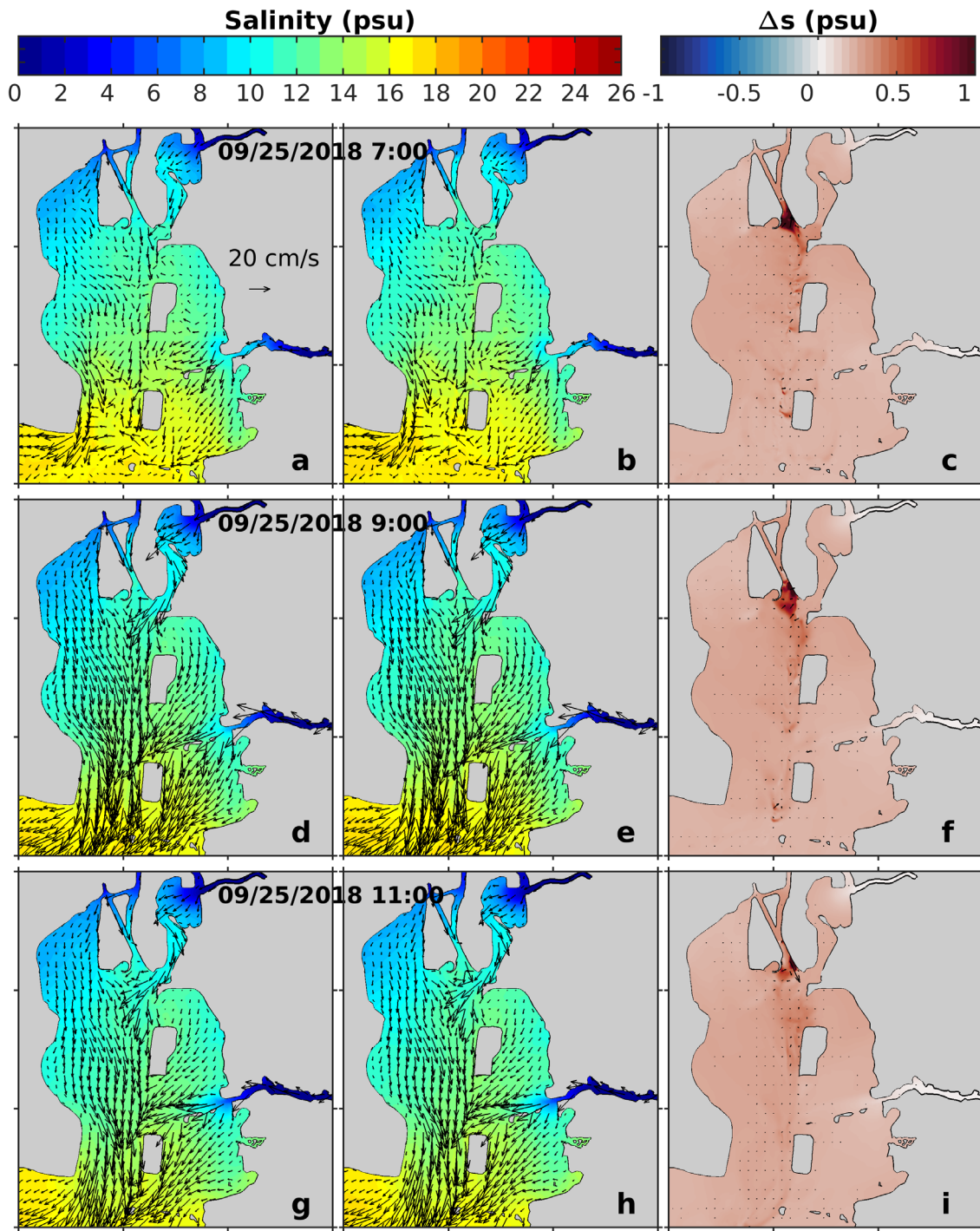
288

289

290

291

**Figure 6.** Instantaneous, near surface layer currents (arrows) and salinity distributions (color coded) during the wet season within Hillsborough Bay sampled at 2 hour intervals simulated by TBCOM, either with the HFCAWTP outfall (left column), or without the HFCAWTP outfall (middle column). The right column shows the differences between the middle and left columns.



292

293 **Figure 7.** Continuation of Figure 6.

294

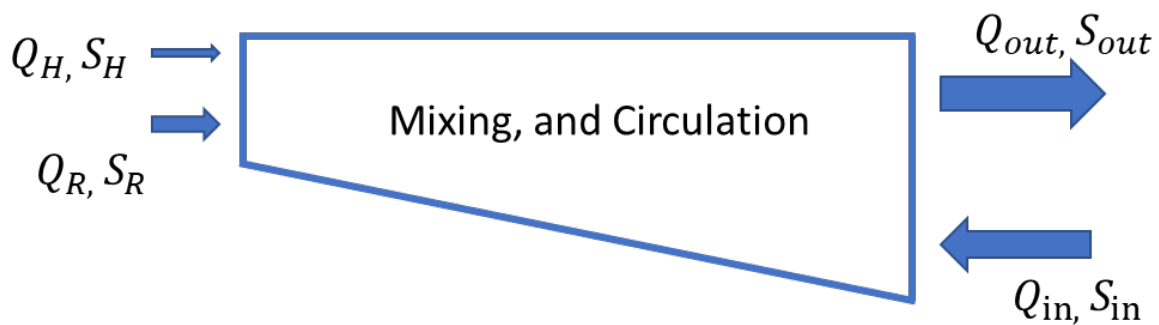
295

296 **5 Estimation of the effect of salinity through Knudsen theorem**

297 The distribution of salinity in an estuary is influenced by advection (the circulation) and  
298 mixing, assuming negligible precipitation and evaporation changes occurring over a short  
299 duration. To simulate these processes the model must be fully three-dimensional, density  
300 dependent and with a mixing parameterization that is also flow dependent (the larger the flow  
301 and the flow gradients, the larger the mixing). TBCOM has these attributes.

302 Despite these complexities, we may crudely estimate the effects of freshwater inflow  
303 modification by using a simplified, mean estuary circulation (the upper layer being directed  
304 seaward and the lower layer landward) construct yielding what is referred to as the Knudsen  
305 theorem (e.g., Knudsen, 1900, MacCready and Geyer, 2010, Burchard et al., 2018) that may be  
306 derived by considering Figure 8. On average, there exists a water volume outflow near the  
307 surface and an inflow at depth ( $Q_{out}$  and  $Q_{in}$ , respectively) at the mouth of the estuary, plus an  
308 inflow of river water ( $Q_R$ ) at the head of the estuary. In a steady balance condition, the salt flux  
309 through the mouth of the estuary is control by the river flux and the exchange flow.

310 Given this theorem, we may ask what the change in the mean salinity of the estuary may  
311 be if amount of the inflowing river water is changed. We can do this by balancing both the mass  
312 of water and the mass of salt with a well-mixed, box model as depicted in the Figure 8.



313  
314 **Figure 8.** Schematic of simplified box model.

315

316 Here,  $Q_R$  is the volume flux of the river,  $Q_H$  is the volume flux of the HFCAWTP,  $Q_{out}$   
317 is the volume flux of upper branch of estuarine circulation out of the estuary,  $Q_{in}$  is the volume  
318 flux of lower branch of estuarine circulation in the estuary. Thus, to balance the mass of water:

319 
$$Q_{out} = Q_{in} + Q_R + Q_H \quad (1)$$

320 If each of these water fluxes contain a certain salinity, then the volume flux of water times the  
321 salinity gives the salt flux. In the steady state these must also balance. Let  $(S_H, S_R, S_{in})$  be the  
322 salinities of the water flowing into the bay and let  $S_{out}$  be the salinity of the water flowing out of  
323 the bay; hence,

324 
$$Q_{out}S_{out} = Q_H S_H + Q_R S_R + Q_{in} S_{in} \quad (2)$$

325 For Hillsborough Bay:  $Q_R = (27.3+27.3+5.7+2.9) \text{ m}^3/\text{s} = 63.2 \text{ m}^3/\text{s}$  and  $S_R = 0$  psu, and for  
326 HFCAWTP:  $Q_H = 3 \text{ m}^3/\text{s}$  and  $S_H = 1$  psu.

327 We assume an average Hillsborough Bay depth of 3 m with equal inflow and outflow  
328 depths of 1.5 m each and the average speed of the estuarine circulation of 0.03 m/s. Further,  
329 taking the width of Hillsborough Bay at its mouth to be 6300 m (from Google Earth), we can  
330 estimate:

331 
$$Q_{in} \approx 1.5\text{m} * 6300\text{m} * 0.03\text{m/s} = 283.5 \text{ m}^3/\text{s}$$

332 
$$Q_{out} \approx Q_{in} + Q_R + Q_H = 349.7 \text{ m}^3/\text{s}$$

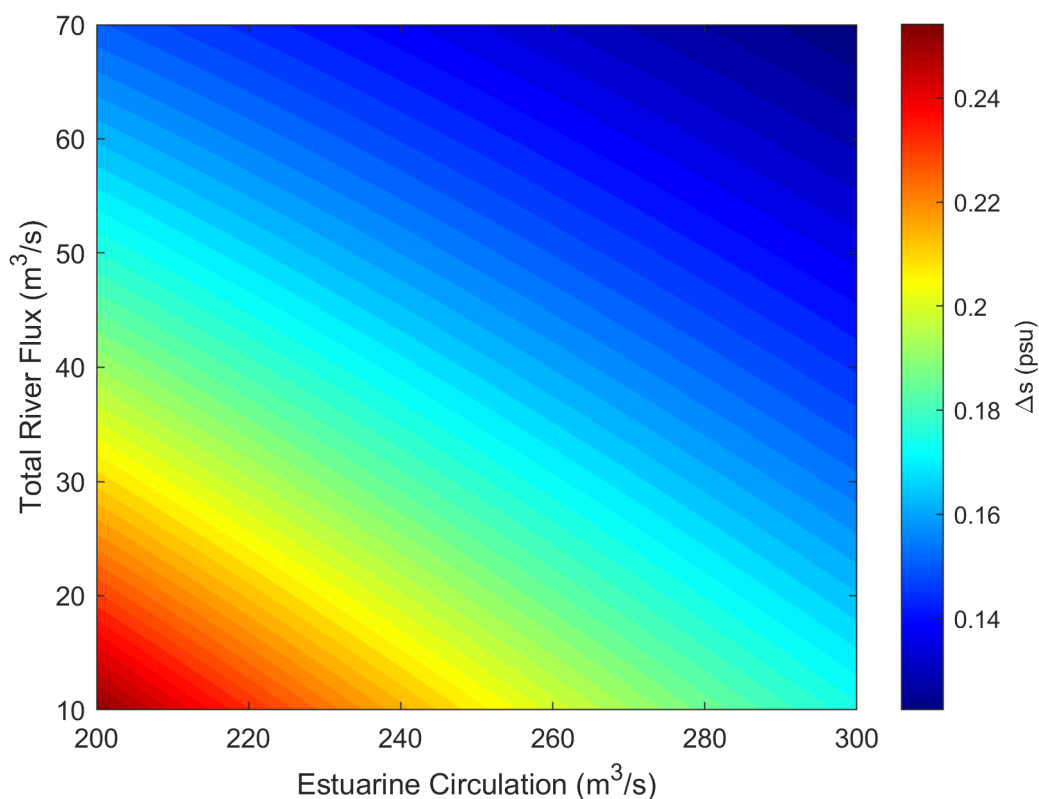
333 Assume the salinity of this landward flux  $S_{in}$  to be 20psu, we can then estimate  $S_{out}$  from  
334 (2):

335 
$$S_{out} = (Q_H S_H + Q_R S_R + Q_{in} S_{in}) / Q_{out}$$

336 Thus, with the HFCAWTP included:  $S_{out} = 16.22$  psu, whereas with the HFCAWTP  
337 excluded:  $S_{out} = 16.35$  psu. The difference between these two estimates amount to:  $\Delta S = 16.35 -$   
338  $16.22 = 0.13$  psu, which is similar to what was estimated from the much more complete TBCOM

339 simulation.

340 The reason for this small change is that neither the volume flux, nor the salinity of the  
341 inflowing water will change much with the HFCAWTP outflow, which is small when compared  
342 with the natural river inflows or with the mean estuary circulation. Moreover, given the flushing  
343 time for Tampa Bay of several months (Zhu et al, 2015b), the transitions from wet to dry seasons  
344 of shorter duration also will not alter the influx through the Hillsborough Bay mouth enough to  
345 significantly modify this finding.



346  
347 **Figure 9.** Change of average salinity ( $\Delta S$ ) Hillsborough Bay under different river flux and  
348 estuarine circulation circumstances due to the removal of HFCAWTP outflow calculated by  
349 Knudsen theorem.

350

351 The river flux can be affected by evaporation, precipitation and human activities. The  
352 estuarine circulation can be affected by wind and tide. In order to have a better estimation of the  
353 influence of HFCAWTP inflow modification on Hillsborough Bay's salinity, the changes of  
354 average salinity in Hillsborough Bay under different river flux and estuarine circulation  
355 conditions assuming 3 m<sup>3</sup>/s HFCAWTP inflow calculated by Knudsen theorem are shown in  
356 Figure 9. We can see that the changes are increased due to the lower river discharge and  
357 estuarine circulation. In the extremely low river flux (10 m<sup>3</sup>/s) and estuarine circulation (200  
358 m<sup>3</sup>/s) case, the change of average salinity in Hillsborough Bay is about 0.26.

## 359 **6 Summary and Conclusions**

360 We applied the Tampa Bay Coastal Ocean Model (TBCOM) to assess the potential  
361 effects of terminating the discharge of treated reclaimed water into the Hillsborough Bay portion  
362 of Tampa Bay at the location of the Howard F. Curren Advanced Wastewater Treatment Plant  
363 (HFCAWTP) outflow. TBCOM is a numerical circulation model that downscales from the deep  
364 ocean, across the continental shelf and into Tampa Bay with veracity sufficiently demonstrated  
365 to justify its utility for addressing salinity and circulation changes owing to the HFCAWTP  
366 discharge being switched on or off.

367 The numerical experiment approach was to consider the HFCAWTP discharge being  
368 either on or off during either wet or dry seasons. The differences for the nontidal circulations and  
369 salinity between the experiments with and without the HFCAWTP outfall during the dry season  
370 are slightly larger when compared with the wet season. This is due the smaller river flux input to  
371 the bay during the dry season. Smaller river flux in dry season makes HFCAWTP flux relatively  
372 important at this period of time compared with wet season. The differences of salinity and  
373 currents are small compared with the tidal variation when investigating the distribution of the

374 near surface instantaneous currents and salinity over about one semidiurnal tidal cycle either  
375 with or without the HFCAWTP outfall.

376 As a check on the numerical experiments, we also considered a simpler, analytical  
377 approach using the relationships between estuarine fresh water inflows and salinity. Through the  
378 Knudsen theorem, the estimated salinity different between two cases is small. This is mainly  
379 because the HFCAWTP outflow is small when compared with the natural river inflows or the  
380 mean estuary circulation. This simple box model derived from Knudsen theorem confirms the  
381 order of the magnitude of the salinity change estimated with the numerical model. For more  
382 precise result and temporal and spatial variation, we still need to rely on the numerical model.

383 In conclusion, the potential reduction of the treated reclaimed water inflow from  
384 HFCAWTP will not significantly affect the circulation or the salinity distributions of  
385 Hillsborough Bay or the larger Tampa Bay. These effects are very localized and minimal when  
386 compared with variations that occur naturally. This finding in Hillsborough Bay by both  
387 numerical and the box model derived from the Knudsen theorem may be applied to water bodies  
388 with similar environmental conditions. A caveat is that the Knudsen theorem approach provides  
389 bulk estimation, versus a site-specific estimation. If the latter is required, then a high-resolution  
390 numerical circulation model is the appropriate estimation tool.

391 Given the application presented herein, plus other recent applications discussed in section  
392 1, TBCOM offers opportunities for a variety of interdisciplinary environmental applications  
393 throughout Tampa Bay, Sarasota Bay, the Intra-Coastal Waterway and all of the connections  
394 between these and the adjacent GOM.

395

396 **Acknowledgments:** Funding was by a work order between the City of Tampa and University of  
397 South Florida to study the impacts on Tampa Bay owing to the Tampa Augmentation Project.  
398 This application was also supported by NOAA/IOOS through the Southeast Coastal Ocean  
399 Observing Regional Association (SECOORA, award NA21NOS0120097), NOAA Office of  
400 Coast Survey through the Center for Ocean Mapping and Innovative Technologies (COMIT,  
401 award NA20NOS4000227), NOAA ECOHAB program (award NA19NOS4780183), State of  
402 Florida Department of Environmental Protection (agreement # AT007), and State of  
403 Florida through FWC/FWRI (agreement # 20035). This work used Stampede2 at TACC  
404 through allocation OCE170007 from the Extreme Science and Engineering Discovery  
405 Environment (XSEDE), which is supported by National Science Foundation grant ACI-1548562  
406 (Towns et al., 2014). We also thank Chuck Weber and Seung Park at Water Department, City of  
407 Tampa for helpful discussions. All of the data used in the analyses are available through the  
408 sources cited in the text.

409  
410  
411  
412



413 **References**

- 414 Aristizábal, M. F., & Chant, R. J. (2015). An observational study of salt fluxes in Delaware Bay.  
415 *J. Geophys. Res. Ocean.* 120(4), 2751-2768.
- 416 Chassignet, E.P., H.E. Hurlburt, E. J. Metzger, O. M. Smedstad, J. A. Cummings, G. R.  
417 Halliwell et al. (2009), US GODAE: global ocean prediction with the HYbrid Coordinate  
418 Ocean Model (HYCOM) *Oceanography* 22(2), 64-75.
- 419 Beck, M. W., Altieri, A., Angelini, C., Burke, M. C., Chen, J., Chin, D. W., ... & Whalen, J.  
420 (2022). Initial estuarine response to inorganic nutrient inputs from a legacy mining  
421 facility adjacent to Tampa Bay, Florida. *Mar. Pollut. Bull.*, 178, 113598.
- 422 Burchard, H., Bolding, K., Feistel, R., Gräwe, U., Klingbeil, K., MacCready, P., ... & van der  
423 Lee, E. M. (2018). The Knudsen theorem and the Total Exchange Flow analysis  
424 framework applied to the Baltic Sea. *Progress in oceanography*, 165, 268-286.
- 425 Chen, C.S., H. Liu, and R. C. Beardsley (2003), An unstructured, finite-volume, three-  
426 dimensional, primitive equation ocean model: Application to coastal ocean and  
427 estuaries, *J. Atmos. Oceanic Technol.*, **20**, 159–186.
- 428 Chen, C., Qi, J., Li, C., Beardsley, R. C., Lin, H., Walker, R., & Gates, K. (2008). Complexity of  
429 the flooding/drying process in an estuarine tidal-creek salt-marsh system: An application  
430 of FVCOM. *J. Geophys. Res. Ocean.* 113(C7).
- 431 Chen, J. (2021). On the Physical Oceanography of Tampa Bay. PhD dissertation, University of  
432 South Florida, St. Petersburg, Florida.
- 433 Chen, J., R. H. Weisberg, Y. Liu, and L. Zheng (2018), The Tampa Bay Coastal Ocean Model  
434 Performance for Hurricane Irma, *Mar Technol Soc J.*, 52(3),33-42,  
435 doi:10.4031/MTSJ.52.3.6.

436 Chen, J., Weisberg, R.H., Liu, Y., Zheng, L. and Zhu J. (2019), On the Momentum Balance of  
437 Tampa Bay, *J. Geophys. Res.: Oceans*. 124, 4492-4510, doi:10.1029/2018JC014890

438 Chen, S. N., & Sanford, L. P. (2009). Axial wind effects on stratification and longitudinal salt  
439 transport in an idealized, partially mixed estuary. *J. Phys. Oceanogr.*, 39(8), 1905-1920.

440 Das, A. (2010). Modeling the impacts of pulsed riverine inflows on hydrodynamics and water  
441 quality in the Barataria Bay estuary.

442 Donlon, C.J., Martin, M., Stark, J., Roberts-Jones, J., Fiedler, E. and Wimmer, W. 2012. The  
443 operational sea surface temperature and sea ice analysis (OSTIA) system. *Remote Sens.*  
444 *Environ.*, 116:140-158.

445 Geyer, W. R. (1993). The importance of suppression of turbulence by stratification on the  
446 estuarine turbidity maximum. *Estuaries*, 16(1), 113-125.

447 Giddings, S. N., & MacCready, P. (2017). Reverse estuarine circulation due to local and remote  
448 wind forcing, enhanced by the presence of along-coast estuaries. *J. Geophys. Res.:*  
449 *Oceans*, 122(12), 10184-10205.

450 Gillanders, B.M., and Kingsford, M.J.A. (2002), Impact of changes in flow of freshwater on  
451 estuarine and open coastal habitats and the associated organisms, *Oceanography and*  
452 *marine biology: an annual review*, 40, 233-309.

453 Gunter, G. (1961), Some relations of estuarine organisms to salinity, *Limnol. Ocean.*, 6(2), 182-  
454 190.

455 Hess, K. (2001), Generation of tidal datum fields for Tampa Bay and the New York Bight,  
456 NOAA Tech. Rep. NOS CS 11, 43 pp., Natl. Ocean Serv., Natl. Oceanic and Atmos.  
457 Admin., Silver Spring, Md.

458 Kang, X., Xia, M., Pitula, J. S., & Chigbu, P. (2017). Dynamics of water and salt exchange at  
459 Maryland Coastal Bays. *Estuar. Coast. Shelf Sci.*, 189, 1-16.

460 Kang, X., & Xia, M. (2022). Stratification variability in a lagoon system in response to a passing  
461 storm. *Limnol. Ocean.*, 67(2), 511-521.

462 Kimmerer, W.J. (2002), Effects of freshwater flow on abundance of estuarine organisms:  
463 physical effects or trophic linkages? *Marine Ecology Progress Series*, 243, 39-55.

464 Knudsen, M. (1900). Ein hydrographischer Lehrsatz. *Hydrogr. Mar. Meteorol.* 28 (7), 316–320  
465 in German

466 Niu, Q., Xia, M., Ludsin, S. A., Chu, P. Y., Mason, D. M., & Rutherford, E. S. (2018). High-  
467 turbidity events in Western Lake Erie during ice-free cycles: Contributions of river-  
468 loaded vs. resuspended sediments. *Limnol. Ocean.*, 63(6), 2545-2562.

469 Liu, Y., Weisberg, R. H., Hubbard, K., Garrett, M., Chen, J., Zheng, L. (2018). Short-term and  
470 seasonal forecasts of harmful algal blooms on the West Florida Shelf. Abstracts (OS33E-  
471 1953) Presented at AGU Fall Meeting, December, 2018, Washington, DC,  
472 <https://ui.adsabs.harvard.edu/abs/2018AGUFMOS33E1953L>

473 Liu, Y., Weisberg, R.H., Zheng, L., Sun, Y., Chen, J. (2021). Nowcast/forecast of the Tampa Bay,  
474 Piney Point effluent plume: a rapid response. Abstract (OS35b-1036) Presented at AGU Fall  
475 Meeting, December, 2021, New Orleans, Louisiana,  
476 <https://ui.adsabs.harvard.edu/abs/2021AGUFMOS35B1036L>

477 MacCready, P., & Geyer, W. R. (2010). Advances in estuarine physics. *Annu. Rev. Mar. Sci.*,  
478 2(1), 35-58.

479 Prandle, D. (1985). On salinity regimes and the vertical structure of residual flows in narrow  
480 tidal estuaries. *Estuar. Coast. Shelf Sci.*, 20(5), 615-635.

481 Qiu, C., & Zhu, J. R. (2013). Influence of seasonal runoff regulation by the Three Gorges  
482 Reservoir on saltwater intrusion in the Changjiang River Estuary. *Cont. Shelf Res.*, 71,  
483 16-26.

484 Sahoo, B., Mao, M., & Xia, M. (2021). Projected changes of water currents and circulation in  
485 Lake Michigan under Representative Concentration Pathways scenarios. *J. Geophys. Res.*  
486 *Ocean.*, 126(5), e2020JC016651.

487 Simpson, J. H., Brown, J., Matthews, J., & Allen, G. (1990). Tidal straining, density currents,  
488 and stirring in the control of estuarine stratification. *Estuaries*, 13(2), 125-132.

489 Towns, J., Cockerill, T., Dahan, M., Foster, I., Gaither, K., Grimshaw, A., Hazlewood, V.,  
490 Lathrop, S., Lifka, D., Peterson, G. D., Roskies, R., Scott, J. R., & Wilkins-Diehr, N.  
491 (2014). XSEDE: Accelerating scientific discovery. *Computing in Science and*  
492 *Engineering*, 16(5), 62– 74. <https://doi.org/10.1109/mcse.2014.80>

493 Virmani, J.I. & Weisberg, R.H. 2005. Relative humidity over the West Florida continental shelf.  
494 *Monthly weather review*, 133(6):1671-1686. <https://doi.org/10.1175/MWR2944.1>.

495 Weisberg, R.H. (1976). The non-tidal flow in the Providence River of Narragansett Bay: A  
496 stochastic Approach to Estuarine Circulation, *J. Phys. Oceanogr.*, 6, 721-734.

497 Weisberg, R.H., and L. Zheng (2006), Circulation of Tampa Bay driven by buoyancy, tides, and  
498 winds, as simulated using a finite volume coastal ocean model, *J. Geophys.*  
499 *Res.*, **111**, C01005, doi:[10.1029/2005JC003067](https://doi.org/10.1029/2005JC003067).

500 Weisberg, R.H., Zheng, L. & Peebles, E. 2014. Gag grouper larvae pathways on the West Florida  
501 Shelf. *Cont. Shelf Res.*, 88:11-23. <https://doi.org/10.1016/j.csr.2014.06.003>

502 Weisberg, R.H., Zheng, L., & Liu, Y. (2016). West Florida Shelf upwelling: Origins and  
503 pathways. *J. Geophys. Res. Ocean.*, 121, 5672– 5681.  
504 <https://doi.org/10.1002/2015JC011384>

505 Weisberg, R.H., Liu, Y., Lembke, C., Hu, C., Hubbard, K., Garrett, M. (2019), The coastal ocean  
506 circulation influence on the 2018 West Florida Shelf *K. brevis* red tide bloom, *J.*  
507 *Geophys. Res. Oceans*, 124, 2501-2512, <https://doi.org/10.1029/2018JC014887>.

508 White, E. D., Messina, F., Moss, L., & Meselhe, E. (2018). Salinity and marine mammal  
509 dynamics in Barataria Basin: Historic patterns and modeled diversion scenarios. *Water*,  
510 10(8), 1015.

511 Xia, M., Craig, P. M., Wallen, C. M., Stoddard, A., Mandrup-Poulsen, J., Peng, M., ... & Liu, Z.  
512 (2011). Numerical simulation of salinity and dissolved oxygen at Perdido Bay and  
513 adjacent coastal ocean. *J. Coastal Res.*, 27(1), 73-86.

514 Xia, M., Mao, M., & Niu, Q. (2020). Implementation and comparison of the recent three-  
515 dimensional radiation stress theory and vortex-force formalism in an unstructured-grid  
516 coastal circulation model. *Estuar. Coast. Shelf Sci.*, 240, 106771.

517 Xie, S., J. Law, R. Russell, T.H. Dixon, C. Lembke, R. Malservisi, ...& J. Chen (2019), Seafloor  
518 geodesy in shallow water with GPS on an anchored spar buoy. *J. Geophys. Res. Solid*  
519 *Earth*. doi:10.1029/2019JB018242

520 Xie, S., Chen, J., Dixon, T. H., Weisberg, R. H., & Zumberge, M. A. (2021). Offshore sea levels  
521 measured with an anchored spar-buoy system using GPS interferometric reflectometry. *J.*  
522 *Geophys. Res. Ocean.*, 126(11), e2021JC017734.

523 Yuan, R., Zhu, J., & Wang, B. (2015). Impact of sea-level rise on saltwater intrusion in the Pearl  
524 River Estuary. *J. Coastal Res.*, 31(2), 477-487.

525 Zheng, L., Chen, C., and Liu, H. (2003). A modeling study of the Satilla River Estuary, Georgia.  
526 I: Flooding-drying process and water exchange over the salt marsh-estuary-shelf  
527 complex. *Estuaries*, 26(3), 651-669.

528 Zheng, L., and R.H. Weisberg (2012), Modeling the west Florida coastal ocean by downscaling  
529 from the deep ocean, across the continental shelf and into the estuaries, *Ocean*  
530 *Modell.*, 48, 10–29, doi:[10.1016/j.ocemod.2012.02.002](https://doi.org/10.1016/j.ocemod.2012.02.002).

531 Zhu, J., R.H. Weisberg, L. Zheng, and S. Han (2015a), Influences of channel deepening and  
532 widening on the tidal and nontidal circulations of Tampa Bay. *Estuaries and*  
533 *coasts*, 38(1), 132-150, doi:[10.1007/s12237-014-9815-4](https://doi.org/10.1007/s12237-014-9815-4).

534 Zhu, J., R.H. Weisberg, L. Zheng, and S. Han (2015b), On the flushing of Tampa Bay. *Estuaries*  
535 *and coasts*, 38(1), 118-131, doi:[10.1007/s12237-014-9793-6](https://doi.org/10.1007/s12237-014-9793-6).

536 Zhu, J., R.H. Weisberg, L. Zheng, and H. Qi (2015c), On the salt balance of Tampa Bay. *Cont.*  
537 *Shelf Res.*, 107, 115-131, doi:[10.1016/j.csr.2015.07.001](https://doi.org/10.1016/j.csr.2015.07.001).

538 Zhu, J., Cheng, X., Li, L., Wu, H., Gu, J., & Lyu, H. (2020). Dynamic mechanism of an  
539 extremely severe saltwater intrusion in the Changjiang estuary in February 2014. *Hydrol.*  
540 *Earth Syst. Sc.*, 24(10), 5043-5056.

541

542

543

544